J Mater Sci (2007) 42:7093–7099
DOI 10.1007/s10853-007-1537-6

Solid-state synthesis of nano-sized $BaTiO_3$ powder with high tetragonality

Sung-Soo Ryu · Dang-Hyok Yoon

Received: 7 August 2006 / Accepted: 19 January 2007 / Published online: 5 May 2007

Abstract A solid-state reaction method was used to synthesize nano-sized, Ca-doped $BaTiO_3$ powder with high tetragonality (=c/a) in order to increase the volumetric efficiency of multilayer ceramic capacitors (MLCCs). The reaction temperatures for three different starting material combinations were examined by thermogravimetric/differential thermal analysis (TG/DTA). Nano-sized starting materials and the mechanochemical activation of the needle-shaped $BaCO_3$ via high-energy milling were effective in decreasing the reaction temperature. In addition, the results showed that the tetragonality of fine Ca-doped $BaTiO_3$ could be enhanced by 2-step heat treatment, consisting of holding at 800 °C for 1 h followed by consecutive heating to the target temperature, without any significant grain growth than that of the conventional 1-step calcination. The synthesized particles heat-treated at 950 and 1,000 °C by 2-step heat treatment were confirmed by characterization to have an average size of 128 and 212 nm, and a tetragonality of 1.0097 and 1.0105, respectively, which are higher tetragonality values than those previously reported for similar sized particles.

S.-S. Ryu
Korea Institute of Ceramic Engineering and Technology, Seoul 153-801, Korea

D.-H. Yoon (✉)
School of Materials Science and Engineering, Yeungnam University, Dae-dong, Gyeongsan, Gyeongbuk 712-749, Korea
e-mail: dhyoon@ynu.ac.kr

Introduction

Since the capacitance of the multilayer ceramic capacitor (MLCC) is proportional to the permittivity of the dielectrics and inversely proportional to the layer thickness, ultra-fine barium titanate ($BaTiO_3$: BT) powders with high tetragonality (=c/a) are required to increase the volumetric efficiency of MLCCs [1, 2]. An MLCC with the highest volumetric efficiency is currently as thin as 1 μm and is comprised of several hundred dielectric layers showing a capacitance higher than 100 μF. For replacement of Ta- and Al-electrolytic capacitors, this thickness is expected to be further reduced [3–6]. Because of the general belief for each sintered layer of MLCC to possess at least 5 grains to ensure reliability [1, 7], BT powder with the average particle size no more than 200 nm is desirable. However, reduced BT particle size is usually accompanied by decrease in both the dielectric constant and the tetragonality due to the size effect [8–12].

BT has been traditionally synthesized by a solid-state reaction between $BaCO_3$ and TiO_2 at temperature above 1,200 °C [1, 9], which generally resulted in a significant amount of agglomeration, poor chemical homogeneity and coarse particle size due to the high temperature calcination [1, 13–15]. This is why liquid phase synthesis methods such as hydrothermal and coprecipitaiton have been widely used in spite of their high cost. However, a few researchers [14–19] have recently succeeded in the synthesis of fine BT powders by using solid-state reaction below 1,000 °C with the help of newly available very fine starting materials and advanced milling facilities such as high energy mills. The mechanochemical activation by heavy milling is the key in this recent process, which alters the physicochemical properties of starting materials. Moreover, such fine starting materials enhance the solid-state reaction due to their

high activity, and hence decrease the reaction temperature and the final particle size [15, 18, 20]. Compared to the conventional ball mills or attrition mills which use a discontinuous operating system, modern high energy mills use a continuous operating system equipped with a high speed rotor turning at up to several thousand rotations per minute (rpm), disc agitators and a cooling system. Their high energy input, along with the use of small grinding media with diameters of 0.05–0.8 mm, enables the production of very small particle sizes in a very short processing time.

Sakabe et al. [4] reported that the Ca-doped BT synthesized by hydrolysis method showed higher dielectric constant and more stable temperature characteristics than pure BT by decreasing the mobility of oxygen vacancies. However, there has been no other report on the synthesis of Ca-doped BT. In this overall perspective, the aim of the present study is to use solid-state reaction for the synthesis of 200 nm-sized Ca-doped BT powder with a tetragonality higher than 1.008 for MLCC application. For this purpose, two main treatments were employed; the previous milling of needle-shaped $BaCO_3$ to enhance the homogeneity, activity and the number of contact points among constituents before the consecutive mixing of starting materials, and the utilization of a 2-step heat treatment to accelerate the reaction by offering enough time for the elimination of CO_2 and the formation of BT crystallite.

Experimental

Commercial $BaCO_3$ powder (Sakai Chemicals, Japan) with an average particle size of 192 nm and a specific surface area of 19 m^2/g, 10% rutile/90% anatase-phased TiO_2 (SDK, Japan) with 25 nm and 50 m^2/g, and $CaCO_3$ (Ube Industry, Japan) with 62 nm and 30 m^2/g, according to the suppliers' data, respectively, were used for the starting materials. In order to check the effects of phase and particle size of TiO_2 on the solid-state reaction temperature, 70% rutile/30% anatase-phased TiO_2 (Ishihara Corp., Japan) with 98 nm and 20 m^2/g, respectively, was also used. The scanning electron microscopy (SEM) morphologies of the starting materials are shown in Fig. 1. Since the as-received $BaCO_3$ powder showed a coarse needle shape compared to the other fine powders with spherical shape as shown in Fig. 1, 40 kg of $BaCO_3$ was milled previously for 20 h before mixing all the starting materials. The milling was performed in an aqueous system using a high-energy mill (LME 4, Netzsch, Germany) with 0.65 mm-diameter ZrO_2 beads and a rotational speed of 1,600 rpm. This milled $BaCO_3$ phase was subsequently dried and crushed.

In order to check the reaction temperature, thermogravimetric/differential thermal analysis (TG/DTA: TGD 9600, TA Instruments) was performed in air for three different combinations of starting materials, as shown in Table 1. A total of 10 mg of each mixture was heated up to 1,100 °C at 3 °C/min under a 0.1 L/min flow of dry air for TG/DTA. Moreover, X-ray diffraction (XRD: RINT 2200, Rigaku using CuK_α line, 40 kV and 40 mA, continuous scan at 4°/min with a collection width of 0.02°) analysis was performed for A-powder to investigate the formation temperature of BT crystallites because A powder showed the lowest reaction temperature based on TG/DTA results. For this test, A-powder (30 g) was heat-treated for 1 min at various temperatures between 600 and 1,000 °C with a heating rate of 15 °C/min and air-quenched directly from the target temperature to room temperature.

The target formulation using A-powder was $(Ba_{0.98}Ca_{0.02})_{1.002}TiO_3$, where the relative molar ratios among the elements were checked and calibrated if needed during the experiments using an X-ray fluorescence (XRF, Simultix 12, Rigaku, Japan) technique. An ammonium salt of polycarboxylic acid (Cerasperse 5468-CF, San Nopco, Korea; 2.2 wt.% with respect to the total ceramic) was added as a dispersant, and the de-ionized water to ceramic ratio was fixed at 1.6/1. After an additional 8 h of milling, 50 kg of A-powder underwent spray drying at 170 °C and pulverization. Samples of this powder (30 g) were taken and exposed to the conventional 1- or 2-step calcination process. Two-step heat treatment was composed of holding at 800 °C for 1 h, followed by consecutive heating to target temperature of 900, 950, or 1,000 °C for 1 h in air. The heating and cooling rates were fixed at 15 °C/min during this calcination process. Characterization using SEM (S-4100, Hitachi), XRD, TG/DTA, specific surface area measurement (BET: ASAP 2010, Micromeritics) and particle size analyzer (PSA: LA-920, Horiba) was performed for the obtained powders. XRD patterns were used to determine the tetragonality, the relative ratio of lattice parameter of c- to a-axis, which was calculated from the peak splitting of (200) and (002) planes for 2θ = 44–46°. Since PSA did not give exact data on the primary particle size due to the necking and agglomeration of the final particles, the average particle size was simultaneously measured using an image analyzer software (SigmaScan, Systat Software, USA) by measuring the lengths of the maximum and minimum diameters for 150 particles based on the SEM micrographs. A total of 15 kg of $(Ba_{0.98}Ca_{0.02})_{1.002}TiO_3$ powder was synthesized by 2-step heat treatment according to the optimum condition based on the above experimental results for MLCC manufacture.

Results and discussion

Most fine $BaCO_3$ powders synthesized by solution technique have a needle shape, as shown in Fig. 1a, which is

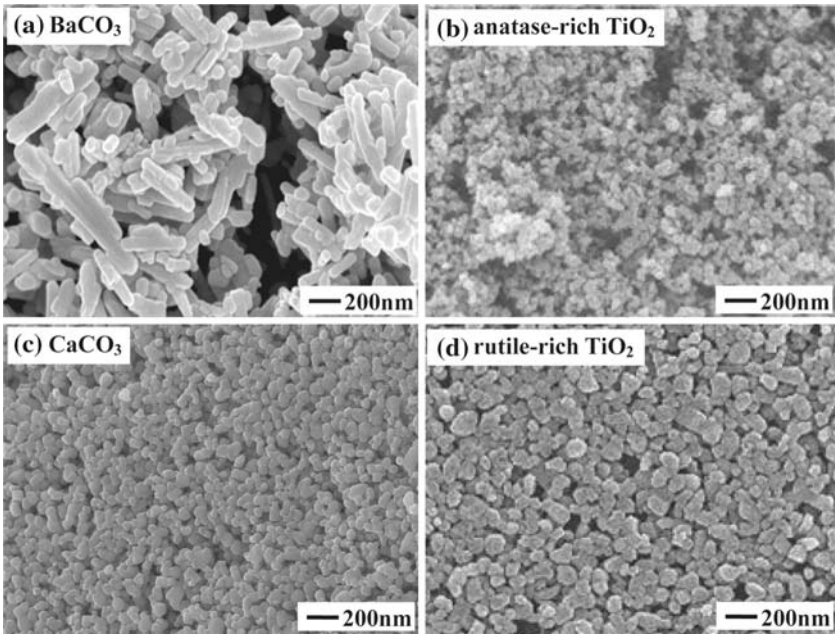

Fig. 1 SEM morphologies of very fine starting materials: (**a**) as-received $BaCO_3$, (**b**) anatase-rich TiO_2, (**c**) $CaCO_3$, and (**d**) rutile-rich TiO_2

Table 1 Combinations of starting materials for TG/DTA analysis

Name	$BaCO_3$	TiO_2	$CaCO_3$
N-powder	As-received	Rutile-rich	As-received
R-powder	20 h milled	Rutile-rich	As-received
A-powder	20 h milled	Anatase-rich	As-received

one of the most serious obstacles for the homogeneous mixing of starting materials in solid-state BT synthesis [13, 21]. To mitigate this problem, $BaCO_3$ powder was therefore milled previously using a high-energy mill, which introduced the additional advantage of decreasing the reaction temperature due to the mechanochemical activation [15–19]. Figure 2a shows the SEM morphology of $BaCO_3$ powder previously milled for 20 h before mixing with TiO_2 and $CaCO_3$. As shown in the SEM image of Fig. 2a, 20-h-milled $BaCO_3$ particles showed a very fine, round-shaped morphology compared to the as-received sample shown in Fig. 1a. The average particle size of $BaCO_3$ decreased from 192 to 90 nm based on the laser scattering PSA measurement, and the initial surface area increased from 19 to 30 m^2/g by 20-h milling. The SEM image of A-powder mixture after an additional 8 h of mixing showed a well-mixed state, as shown in Fig. 2b.

TG/DTA results with a heating rate of 3 °C/min in air for three different combinations of starting materials are represented in Fig. 3, showing the drastic weight loss between 600 and 900 °C. Since the amount of $CaCO_3$ in the mixture was extremely small, the TG/DTA result mainly reflected the weight loss from $BaCO_3$ and TiO_2. The DTA endothermic peak near 650 °C seemed to correspond to the direct formation of BT from the solid-state reaction of $BaCO_3$ and TiO_2 rather than the decomposition of the $BaCO_3$ based on the recent reports [17, 22]. Even though Beauger et al. [23] and Brzozowski and Castro [15] suggested the previous decomposition of the $BaCO_3$ before solid-state reaction, Buscaglia et al. [17] and Lotnyk et al. [22] recently observed the direct solid-state reaction of $BaCO_3$ and TiO_2 at this temperature range. The relative size of endothermic peak and the corresponding weight loss at ≈650 °C increase in the order of A-, R- and

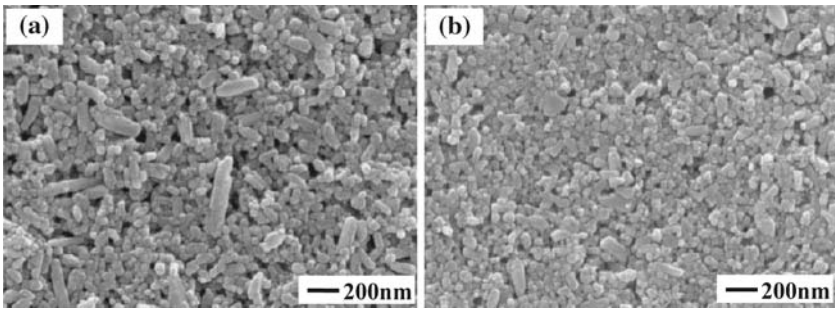

Fig. 2 SEM morphologies of (**a**) the 20-h pre-milled $BaCO_3$ and (**b**) the well-mixed A-powder with an additional 8 h of mixing

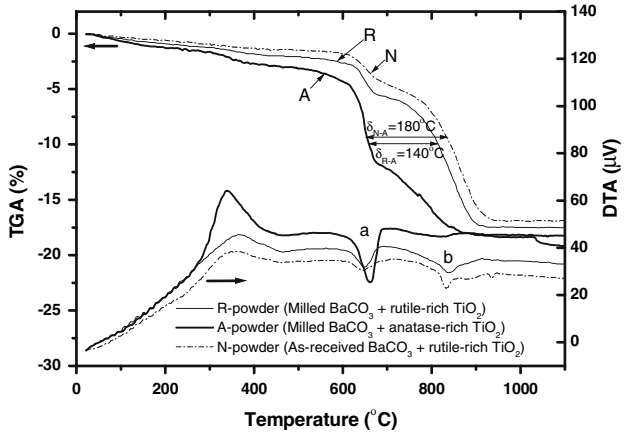

Fig. 3 TG/DTA results for three different combinations of starting materials in air

N-powders. Therefore, this phenomenon can be explained by the effects of fine anatase-rich TiO_2 phase and the previous milling of $BaCO_3$. Regarding the effect of TiO_2 phase, one can estimate that the anatase phase with lower density (3.90 g/cm^3) and larger surface area (50 m^2/g) has a higher activity for solid-state reaction than the rutile one with higher density (4.23 g/cm^3) and smaller surface area (20 m^2/g) [24]. Since the anatase to rutile transformation spontaneously occurs at the temperature above 750 °C [25], the phase transformation of TiO_2 phase does not affect in this temperature range. The reaction temperature reduction effect of $BaCO_3$ milling was smaller than that of fine anatase TiO_2, which can be explained from the weight loss differences among the three types of powders up to 900 °C. Even though the weight loss between 600 and 900 °C was ≈14% for all mixtures, A-powder showed the fastest loss rate among 3 types of mixtures, which suggests the importance of starting materials in the reduction of reaction temperature. The exothermic DTA peak and a small weight loss near 350 °C seemed to be related with the removal of hydroxyl ions in the starting materials. The endothermic peak near 650 °C (peak a) was due to the formation of $BaTiO_3$ while that of near 840 °C (peak b) was due to the $BaCO_3$ phase transition from γ to β phase [15]. Since most of the $BaCO_3$ phase in A-powder was consumed for BT formation near 650 °C, the endothermic peak of this powder at 650 °C was large while the peak due to $\gamma \rightarrow \beta$ transition near 840 °C was insignificant compared to that of R- or A-powder.

According to the previous reports [15, 17, 23], BT is easily formed at the surface of TiO_2 particles. When the surface BT layer is formed, the kinetics is governed by the barium and oxygen ion diffusion through this layer into the virgin TiO_2 phase. Due to the excess of these ions at the surface layer, Ba_2TiO_4 phase is generally formed initially [13, 15, 17, 19, 20, 26]. Homogeneous BT particles are

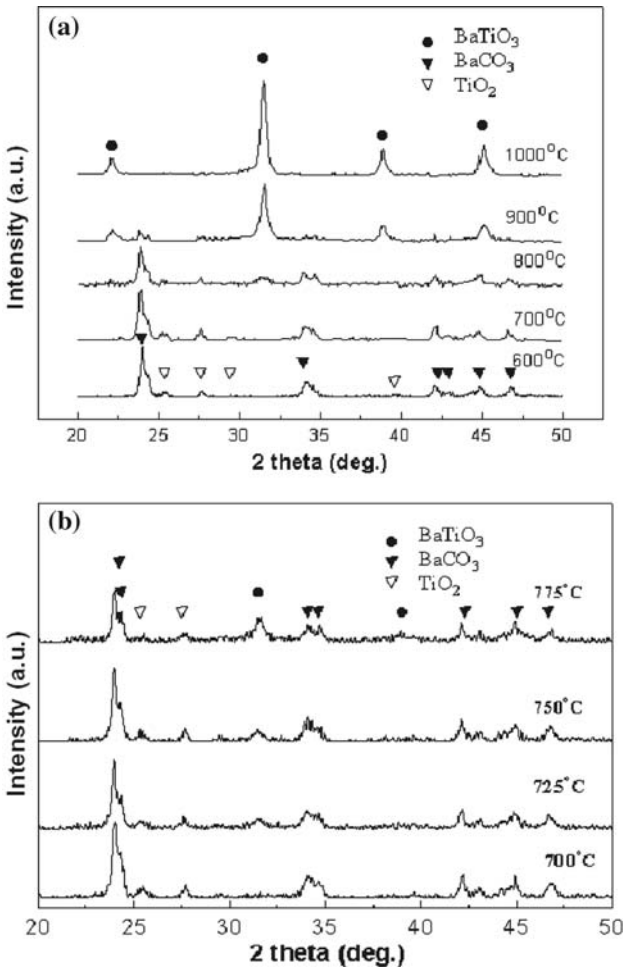

Fig. 4 XRD patterns for A-powder quenched from different temperatures: (**a**) between 600 and 1,000 °C with a 100 °C step and (**b**) between 700 and 775 °C with a 25 °C step

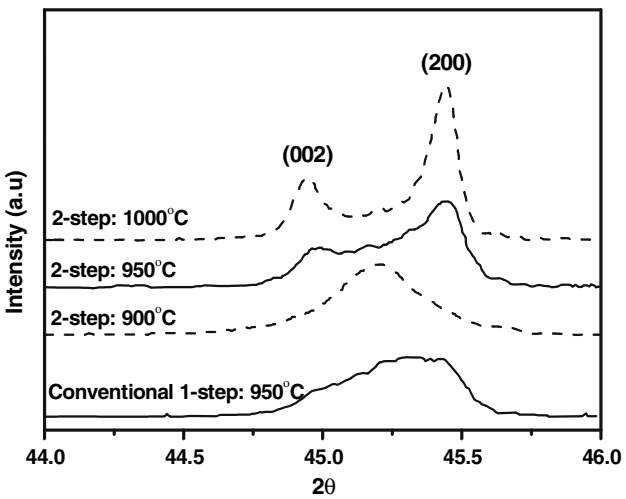

Fig. 5 XRD patterns of $BaTiO_3$ powders synthesized at different temperatures using 2-step heat treatment for 2θ = 44–46°. The peak of $BaTiO_3$ prepared by conventional 1-step calcination at 950 °C is included for comparison

formed gradually by the reaction between Ba_2TiO_4 and TiO_2 due to the continuous diffusion. This reaction mechanism indicates that fine anatase TiO_2 with loose structure, i.e., low density, and large surface area enhances BT formation by decreasing both the diffusion length and the activation energy for the diffusion, which is consistent with our findings. Therefore, the size of the final BT is expected to be primarily determined by the phase and size of starting TiO_2. Moreover, very fine $BaCO_3$ particles may further assist by increasing the contact points with other starting materials and their own easy decomposition.

Figure 4 shows the XRD patterns of heat-treated A-powder quenched from various temperatures (a) between 600 and 1,000 °C with a step of 100 °C and (b) between 700 and 775 °C with a step of 25 °C, which were performed to check the more precise onset temperature for BT formation. According to Fig. 4a, BT peaks start to appear from 800 °C and turn into almost pure BT phase at 900 °C. Figure 4b shows that the BT phase starts to form at 725 °C which is slight higher than the results of TG/DTA (≈650 °C) due to the different experimental conditions of XRD experiment. No significant amount of intermediate $BaTi_2O_4$ phase was detected in our experiments although many authors have observed this phase during the solid-state reaction of BT [13, 15, 17, 19, 20, 26]. However, a few researchers did not observe $BaTi_2O_4$ phase during the solid-state BT synthesis when, as in this study, the anatase-rich nano TiO_2 was used [17, 27].

Figure 5 shows the XRD patterns for (002) and (200) planes of synthesized BT from A-powder after heat treatment at 900, 950 and 1,000 °C for 1 h by 2-step heat treatment along with that of the powder prepared by conventional 1-step heating at 950 °C for comparison. The calculated tetragonality for the 2-step treated BT powder was higher (c/a = 1.0097) than that for conventional-heated powder (c/a = 1.0051), as indicated by the peak separation between (002) and (200) planes after heat treatment at 950 °C. This confirmed the higher tetragonal

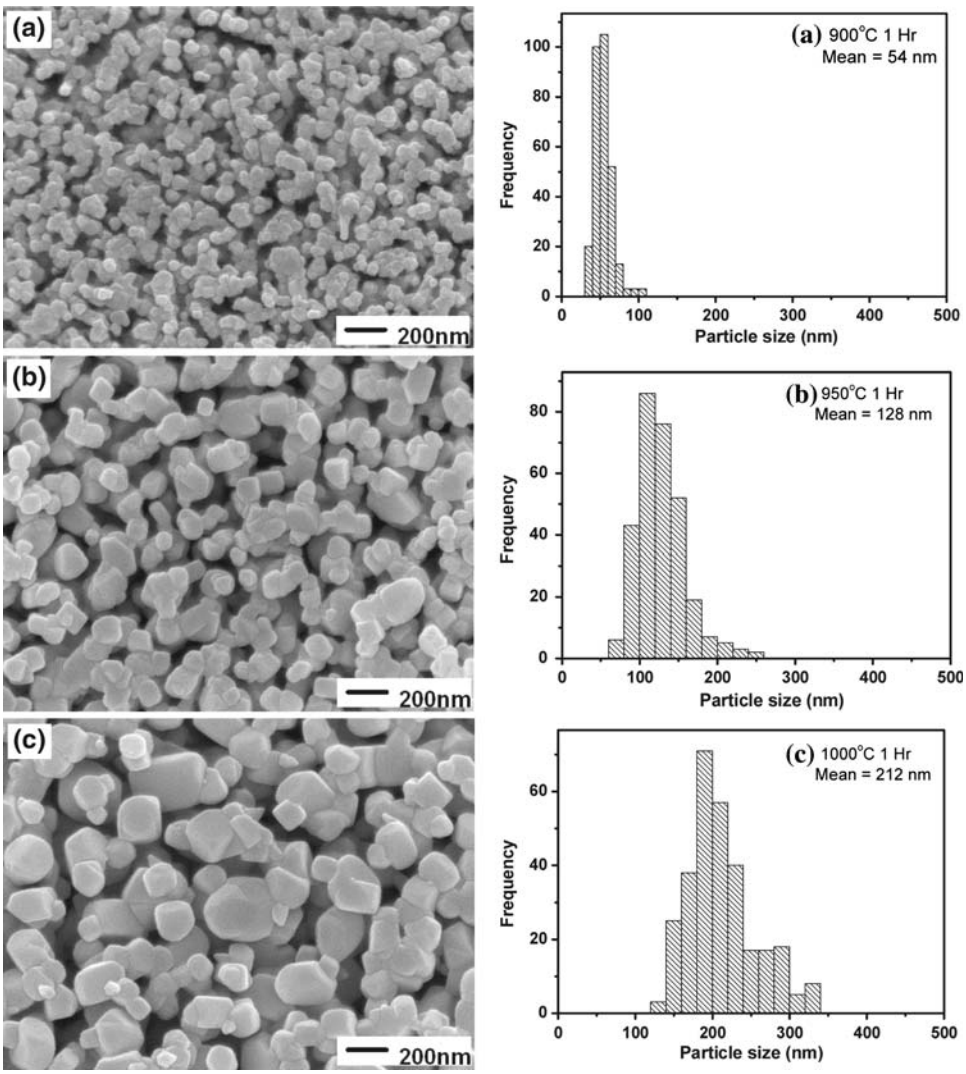

Fig. 6 SEM morphologies and the corresponding particle size distributions of $BaTiO_3$ synthesized from A-powder by 2-step heat treatment at (**a**) 900, (**b**) 950, and (**c**) 1,000 °C in air

phase of the 2-step heat treatment and its greater effectiveness in acquiring high tetragonality compared to the conventional heating. A holding temperature of 800 °C for the 2-step heat treatment was decided based on the TG/DTA result by considering the onset temperature of BT formation and measuring condition, and the XRD data where the nanocrystalline cubic BT was formed. Even though the weight loss of A-powder due to BT formation has almost occurred up to 800 °C, based on Fig. 3, it was measured in flowing dry air with a small sample amount and a 3 °C/min of slow heating rate. The BT formation temperature for a large batch and a 15 °C/min heating rate must be higher than that of the TG/DTA condition in a furnace without gas flow due to the high CO_2 partial pressure. By holding the temperature at 800 °C for 1 h, time is offered for CO_2 elimination and for cubic BT crystallite formation, which resulted in the acceleration of the forward reaction of the following reaction equation by Le Chatelier's principle and the enhancement of tetragonality simultaneously.

$$BaCO_3(s) + TiO_2(s) \rightarrow BaTiO_3(s) + CO_2(g)$$

Figure 6 shows the SEM morphologies of BT powders synthesized at various temperatures by 2-step heat-treatment, along with the particle size distributions measured by image analyzer software. Characterization confirmed an average particle size of 54, 128 and 212 nm, a specific surface area of 13.50, 6.32 and 4.23 m^2/g, and a tetragonality of 1.0000, 1.0097 and 1.0105 for the powders heat-treated at 900, 950 and 1,000 °C, respectively. Laser scattering PSA method showed the D_{50} values of 102, 189 and 301 nm for the corresponding powders, respectively, indicating the mild necking or agglomeration after heat treatment. This synthesized powder was exposed to the neck-breaking process at mild milling condition for further MLCC fabrication.

Table 2 summarizes the recently reported research results of synthesized BT characteristics, including particle sizes and corresponding tetragonality values. The 2-step heat treatment presented in this research exhibited higher tetragonality with finer BT particle size than any other reports. This was due to the use of very fine starting materials, including the previous milling of $BaCO_3$ and utilization of fine anatase-rich TiO_2, and the application of 2-step heat treatment process. The grain growth which inevitably occurs during the high temperature treatment of solid-state BT synthesis could also be minimized by decreasing the reaction temperature.

Table 2 Recent research results of synthesized $BaTiO_3$ characteristics

Researcher	Heat treatment temperature (°C)	Particle size (nm)	Tetragonality (=c/a)	Preparation method
Uchino et al. [9]	–	single crystal	1.0095	Single crystal
	–	120	Cubic	Hydrothermal
	–	200	1.006	Coprecipitation
	–	300	1.009	Solid-state reaction
Sakabe et al. [8]	1,000	290	1.008	Hydrolysis
Kong et al. [14]	1,100	–	Cubic	Hydrothermal
	1,150	3,000	1.01	
Maison et al. [28]	950	230	1.0080	Catecholate process
	1,000	240	1.0086	
	1,100	400	1.0098	
Chen and Chen [29]	900	–	Cubic	Hydrothermal
	1,150	–	1.0105	
Ando et al. [19]	900	–	Cubic	Solid-state reaction
Kown and Yoon [21]	800	<170	Cubic	Hydrothermal
	950	335	1.0105	
Sakabe et al. [4]	1,050	200	1.0095	Hydrolysis (Ca-doped $BaTiO_3$)
Tsurumi et al. [30]	–	125	1.0067	Solid-state reaction (Commercial powders)
	–	130	1.0081	
	–	158	1.0084	
	–	194	1.0097	
This research	900	54	Cubic	Solid-state reaction (Ca-doped $BaTiO_3$)
	950	128	1.0097	
	1,000	212	1.0105	

Conclusions

Despite the great research attention over the last decade on increasing the volumetric efficiency of MLCCs by increasing the number of layers and decreasing the dielectric thickness, electrolytic capacitors using Ta and Al still occupy the high capacitance region beyond 100 μF. In order to replace these Ta- and Al-electrolytic capacitors by MLCCs, continuous technical innovations are required, including the development of very fine BT powder with high tetragonality. For this purpose, very fine Ca-doped BT powders with high tetragonality were synthesized by solid-state reaction in this experiment. The use of mechano-chemically activated $BaCO_3$ via high-energy milling and nano-sized anatase-rich TiO_2 were effective in decreasing the reaction temperature. In addition, the 2-step heat-treated particles showed higher tetragonality than those treated with conventional 1-step calcination process, without any significant grain growth. Characterization confirmed an average particle size of 128 and 212 nm, and a tetragonality of 1.0097 and 1.0105 for the BT powders heat-treated at 950 and 1,000 °C by 2-step heat treatment, respectively.

Acknowledgements This work was supported by Pohang National Center for Nanomaterials Technology. The authors would like to thank Dr. K. H. Hur, Mr. H. S. Jung and Mr. D. S. Lee at Samsung Electro-Mechanics Co. for their considerable cooperation.

References

1. Yoon DH, Lee BI (2002) J Ceram Proc Res 3:41
2. Merz WJ (1949) Phys Rev 76:1221
3. Kwon SW, Yoon DH (2006) Ceram Int (in press)
4. Sakabe Y, Wada N, Hiramatsu T, Tonogaki T (2002) Jpn J Appl Phys 41:6922
5. Wada S, Yasuno H, Hoshina T, Nam SM, Kakemoto H, Tsurumi T (2003) Jpn J Appl Phys 42:6188
6. Kishi H, Mizuno Y, Chazono H (2003) Jpn J Appl Phys 42:1
7. Sakabe Y (2000) In: Jean JH, Gupta TK, Nair KM, Niwa K (eds) Ceramic transactions, vol 97. American Ceramic Society, OH, p 1
8. Sakabe Y, Wada N, Hamaji Y (1998) J Korean Phys Soc 32:S260
9. Uchino K, Sadanaga E, Hirose T (1989) J Am Ceram Soc 72:1555
10. Begg BD, Rvance E, Nowotny J (1994) J Am Ceram Soc 77:3186
11. Vivekanandan R, Kutty TRN (1989) Powder Tech 57:181
12. Arlt G, Hennings D, With GD (1985) J Appl Phys 58:1619
13. Hennings DFK, Schreinemacher BS, Schreinemacher H (2001) J Am Ceram Soc 84:2777
14. Kong LB, Ma J, Huang H, Zhan RFG, Que WX (2002) J Alloys Compos 337:226
15. Brzozowski E, Castro MS (2003) Thermochim Acta 398:123
16. Gomez-Yanez C, Benitez C, Balmori-Ramirez H (2000) Ceram Int 26:271
17. Buscaglia MT, Bassoli M, Buscaglia V (2005) J Am Ceram Soc 88:2374
18. Berbenni V, Marini A, Bruni G (2001) Thermochim Acta 374:151
19. Ando C, Yanagawa R, Chazono H, Kishi H, Senna M (2004) J Mater Res 19:3592
20. Brzozowski E, Castro MS (2000) J Eur Ceram Soc 20:2347
21. Kwon SW, Yoon DH (2006) J Eur Ceram Soc 27:247
22. Lotnyk A, Senz S, Hesse D (2006) Solid State Ionics 177:429
23. Beauger A, Mutin JC, Niepce JC (1983) J Mater Sci 18:3543, DOI: 10.1007/BF00540726
24. O'neil MJ, Smith A, Heckelman PE, Obenchain JR, Gallipeau JAR, D'arecca MA, Budavari S (2001) In The Merck Index. MERCK & CO, Inc, NJ, p 9549
25. Levin EM, Mcmurdie HF (1975) In: Reser MK (ed) Phase diagrams for ceramists. American Ceramic Society, Westerville, OH, p 4258
26. Felgner KH, Muller T, Langhammer HY, Abicht HP (2004) Mater Lett 58:1943
27. Shaikh AS, Vest GM (1986) J Am Ceram Soc 69:682
28. Maison W, Kleeberg R, Heimann RB, Phanichphant S (2003) J Eur Ceram Soc 23:127
29. Chen KY, Chen YW (2004) Powder Tech 41:69
30. Tsurumi T, Sekine T, Kakemoto H, Hoshina T, Nam SM, Yasuno H, Wada S (2006) J Am Ceram Soc 89(4s):1337